Relaxin-3: Improved Synthesis Strategy and Demonstration of Its High-Affinity Interaction with the Relaxin Receptor LGR7 Both In Vitro and In Vivo †

15 AUTHORS, INCLUDING:

Stan Bastiras
Hospira
15 PUBLICATIONS   258 CITATIONS

SEE PROFILE

Tania Ferraro
The Florey Institute of Neuroscience and Men…
27 PUBLICATIONS   1,034 CITATIONS

SEE PROFILE

Sherie Ma
The Florey Institute of Neuroscience and Men…
33 PUBLICATIONS   767 CITATIONS

SEE PROFILE

Chrishan S Samuel
Monash University (Australia)
132 PUBLICATIONS   3,537 CITATIONS

SEE PROFILE

Relaxin-3: Improved Synthesis Strategy and Demonstration of Its High-Affinity Interaction with the Relaxin Receptor LGR7 Both *In Vitro* and *In Vivo*[†]

Ross A. D. Bathgate,[‡] Feng Lin,[‡] Nicola F. Hanson,[‡] Laszlo Otvos, Jr.,[§] Angelo Guidolin,[‖] Chris Giannakis,[‖] Stan Bastiras,[‖] Sharon L. Layfield,[‡] Tania Ferraro,[‡] Sherie Ma,[‡] Chongxin Zhao,[‡] Andrew L. Gundlach,[‡] Chrishan S. Samuel,[‡] Geoffrey W. Tregear,[‡] and John D. Wade*,[‡]

Howard Florey Institute, University of Melbourne, Melbourne, Victoria 3010, Australia, The Wistar Institute, 3601 Spruce Street, Philadelphia, Pennsylvania 19104, and BresaGen Ltd., Post Office Box 259 Rundle Mall, Adelaide, South Australia 5000, Australia

ABSTRACT: Relaxin-3 is a member of the human relaxin peptide family, the gene for which, *RLN3*, is predominantly expressed in the brain. Mapping studies in the rodent indicate a highly developed network of *RLN3*, *RLN1*, and relaxin receptor-expressing cells in the brain, suggesting that relaxin peptides have important functional roles in the central nervous system. A regioselective disulfide-bond synthesis protocol was developed and used for the chemical synthesis of human (H3) relaxin-3. The selectively S-protected A and B chains were combined by stepwise formation of each of the three insulin-like disulfides via aeration, thiolysis, and iodolysis. Judicious positioning of the three sets of S-protecting groups was crucial for acquisition of synthetic H3 relaxin in a good overall yield. The activity of the peptide was tested against relaxin family peptide receptors. Although the highest activity was demonstrated on the human relaxin-3 receptor (GPCR135), the peptide also showed high activity on relaxin receptors (LGR7) from various species and variable activity on the INSL3 receptor (LGR8). Recombinant mouse prorelaxin-3 demonstrated similar activity to H3 relaxin, suggesting that the presence of the C peptide did not influence the conformation of the active site. H3 relaxin was also able to activate native LGR7 receptors. It stimulated increased MMP-2 expression in LGR7-expressing rat ventricular fibroblasts in a dose-dependent manner and, following infusion into the lateral ventricle of the brain, stimulated water drinking in rats, activating LGR7 receptors located in the subfornical organ. Thus, H3 relaxin is able to interact with the relaxin receptor LGR7 both *in vitro* and *in vivo*.

The concept of the relaxin peptide family is now firmly established (*1, 2*). Hence, in humans, there are seven relaxin family peptide genes including *RLN1*, *RLN2*, and *RLN3*, the genes for H1, H2, and H3 relaxins, respectively, together with the insulin-like peptide genes *INSL3−6*, which encode the peptides INSL3, INSL4, INSL5, and INSL6. In most other mammals, there are only two *RLN* genes, encoding relaxin and relaxin-3. The *RLN1* gene in these species is equivalent to the *RLN2* gene in humans and higher primates and encodes the relaxin peptide, which is expressed by the corpus luteum and/or placenta and has a key role in reproductive processes (*3, 4*). The *RLN3* gene was discovered only recently, and it has been demonstrated to be the ancestral gene for the relaxin peptide family (*1, 2*). Hence, relaxin-3 orthologues have been identified in the genomes of all mammals and is the sole relaxin family peptide gene found in the genomes of various fish species, frog, and chicken.

The function of the relaxin-3 peptide is unknown. However, in stark contrast to the relaxin peptide, its highest expression is in the brain. Hence, relaxin-3 mRNA expression is highest in the human brain as indicated by RT-PCR (*5*), in the rat (*6*), and mouse (*7*) brain by Northern blotting, and one of the zebrafish relaxin-3 orthologues is highly represented in brain expressed sequence tag (EST) databases (*8*). In both mouse and rat brain, relaxin-3 mRNA is abundantly expressed in a small nucleus called the nucleus incertus (NI),[1] which is located in the caudoventral regions of the pontine periventricular gray, adjacent to the ventromedial border of the dorsal tegmental nucleus (*6, 7*). Recent studies indicate that the levels of rat relaxin-3 mRNA in the NI are increased in response to stress, indicating that neurons expressing

[1] Abbreviations: BLA, basolateral amygdala; CD, circular dichroism; CRF, corticotropin-releasing factor; Cx, cerebral cortex; DMF, *N*,*N*′-dimethylformamide; DPDS, 2,2′-dipyridyl disulfide; HBTU, 2-(1H-benzotrazole-1-yl)-1,1,3,3-tetramethylronium hexafluorophate; LGR, leucine-rich repeat containing G-protein coupled receptor; GPCR, G-protein coupled receptor; MALDI−TOF, matrix-assisted laser desorption time-of-flight; MMP-2, matrix metalloproteinase-2; NI, nucleus incertus; PVN, paraventricular nucleus; RP-HPLC, reversed-phase high-pressure liquid chromatography; SALPR, somatostain- and angiotensin-like peptide receptor; TES, triethylsilane; TGF-β, transforming growth factor β; TFA, trifluoroacetic acid; TFMSA, trifluoromethanesulfonic acid; SFO, subfornical organ.

	1	5	10	15	20	25

Human 1   R P Y V A L F E K C C L I G C T K R S L A K C
Human 2   Z L Y S A L A N K C C H V G C T K R S L A R C
Human 3   D V L A G L S S S C C K W G C S K S E I S S C

Human 3   R A A P Y G V R L C G R E F I R A V I F T C G G S R W
Human 2   D S W M E E V I K L C G R E L V R A Q I A I C G M S T W S
Human 1   K W K D D V I K L C G R E L V R A Q I A I C G M S T W S

	1	5	10	15	20	25

FIGURE 1: Predicted primary structure of H3 relaxin. The primary structures of H1 and H2 relaxins are shown for a comparison. The disulfide-bond connectivities are identical to insulin and are as follows (using H3 relxin chain numbering): A chain cysteines, 10 and 15; A chain, 11 and B chain, 11; and A chain, 24 and B chain, 23.

relaxin-3 may have a role in the stress response (9). An additional recent study has indicated that relaxin-3 projections to the paraventricular nucleus (PVN) may have a novel role in appetite regulation (10). These studies combined with the remarkable sequence conservation of the relaxin-3 peptide from fish to mammals suggest that relaxin-3 may have very important central functions.

In contrast to the receptors for the related peptides, insulin, and insulin-like growth factors 1 and 2, which are protein tyrosine kinases (11), the receptors for relaxin family peptides are members of two unrelated branches of the G-protein coupled receptor (GPCR) family (12). Leucine-rich-repeat containing G-protein coupled receptor 7 (LGR7) is the receptor for relaxin (13), whereas LGR8 is the receptor for INSL3 (14). Although relaxin-3 will also interact with LGR7 as well as LGR8 in some species (12), its native receptor is GPCR135, also known as the somatostatin- and angiotensin-like peptide receptor (SALPR) (5). A related receptor GPCR142 (GPR100) will also bind relaxin-3 (15) but is likely the native receptor for INSL5 (16). GPCR135 is expressed abundantly in the hypothalamus with discrete expression in the paraventricular nucleus of the hypothalamus and supraoptic nucleus as well as in the cortex, septum, and preoptic areas (5, 17). No other member of the relaxin peptide family binds to this receptor, indicating strongly that relaxin-3 has as yet unidentified specific neurological functions via actions at GPCR135. LGR7 is also expressed in the brain (18, 19), and it is therefore possible that relaxin-3 exerts its actions in the brain via multiple GPCRs.

The native relaxin-3 peptide consists of a 24-residue A chain and a 27-residue B chain that are derived by enzymatic processing of a 66-residue C peptide and contain the characteristic insulin intra- and intermolecular disulfide-bond connectivities (Figure 1). Importantly, the B chain contains an R-X-X-X-R-X-X-I cassette that is the primary active site for characteristic relaxin activity (20). There is a very high degree of sequence homology between the A and B chains of relaxin-3 within species, whereas it is much lower between each of the other human relaxins (7). Little is known about the structural and physicochemical differences between the human relaxins and the possible influences that these have on the scope and specificity of biological activity. Furthermore, its structural and compositional complexity has thus far limited recombinant DNA-derived production of significant quantities of peptide for detailed physicochemical analysis as well as *in vitro* and *in vivo* studies. Consequently,

in the present paper, we report the solid-phase chemical synthesis protocol for the preparation of large amounts of H3 relaxin for a comparison with recombinantly produced mouse prorelaxin-3 as well as the further detailed characterization of its activity on LGR7 receptors both *in vitro* and *in vivo*.

EXPERIMENTAL PROCEDURES

Solid-Phase Peptide Synthesis. Each of the selectively S-protected A and B chains were assembled as either their C-terminal acids or amides using the continuous flow Fmoc solid-phase synthesis methodology essentially as previously described (21). The solid support was appropriately C-terminal amino-acid-linked PAC PEG-PS for the preparation of C-terminal peptide acids or Fmoc-PAL PEG-PS (PerSeptive Biosystems, Framingham, MA) for the preparation of peptide amides, and 2-(1H-benzotrazole-1-yl)-1,1,3,3-tetramethylronium hexaflurophosphate (HBTU)-activated Fmoc amino acids were used throughout. Amino acid side-chain protection was afforded by the following: Arg, Pbf; Asn and Gln, Trt; Asp and Glu, O-Bu^t; His, Trt; Lys, Boc; and Ser and Thr, Bu^t. For the A-chain peptide, S protection was afforded by Trt (Cys^{10,15}), Acm (Cys^{24}), and Bu^t (Cys^{11}). For the B chain, Trt (Cys^{10}) and Acm (Cys^{24}) were used. All amino acid derivatives were purchased from Auspep (Melbourne, Australia). No repeat couplings were carried out. N$^\alpha$-Fmoc deprotection was with 20% piperidine in *N,N'*-dimethylformamide (DMF). The assembly of both the A- and B-chain peptides commenced on 0.6 and 0.2 mmol scales, respectively, using a 4-fold excess of activated amino acid and 30 min coupling times. After acylation and deprotection of the final residues, cleavage from the solid supports and side-chain deprotection was achieved by a 2.5-h treatment of the two separate peptide resins with trifluoroacetic acid (TFA) and, for the B chain, in the presence of phenol, thioanisole, ethanedithiol, and water (82.5:5:5:2.5: 5, v/v/v/v/v) with a few drops of triethylsilane (TES). For the A chain, cleavage was effected with TFA in the presence of ethanedithiol, water, and TES (95:2:2:1). The resulting crude peptides were subjected to preparative reversed-phase high-performance liquid chromatography (RP-HPLC) on a Vydac C18 column (Hesperia, CA) using a 1%/min gradient of CH$_3$CN in 0.1% aqueous TFA.

A-Chain Intramolecular Disulfide Oxidation. Crude cleaved [Cys^{10,15}(*S*-thiol), Cys^{11}(But), and Cys^{24}(Acm)] A chain (976

mg, 376.7 μmol) was dissolved in 0.1 M Gly-NaOH at pH 8.5, (2.81 mL) and to this was added 1 mM 2,2′-dipyridyl disulfide (DPDS) in MeOH (45 mL, 45 μmol) (*21*). Oxidation was complete after 2 h as monitored by analytical RP-HPLC. The solution was acidified by the addition of neat TFA, and then the peptide was isolated by preparative RP-HPLC and subsequent freeze-drying to give 202.6 mg (78.3 μmol) of purified [Cys[11](Acm) and Cys[24](But)] A chain.

[Cys[11](Pyr) and Cys[24](Acm)] A Chain. Intramolecular disulfide-bonded [Cys[11](But) and Cys[24](Acm)] A chain (202 mg, 78 μmol) was converted to the Cys[24] *S*-pyridinylsulfenyl form by treatment with DPDS in neat TFA (5.0 mL) containing thioanisole (0.5 mL) chilled to $\leq$0 °C, and then 5.0 mL of trifluoromethanesulfonic acid (TFMSA)/TFA (1: 5, v/v) was added and stirred for 20−30 min while maintaining the temperature at or below 0 °C. The peptide was then precipitated in ether, and the pellet was suspended in 6 M GdHCl at pH 8.0 for purification. The target peptide was isolated by preparative RP-HPLC to give 71.7 mg (34.7%). To help improve yields, the pellet may instead be suspended in 20% aqueous HOAc and loaded onto a Sephadex G25 (fine) column for size-exclusion separation.

Combination of [Cys[11](Pyr) and Cys[24](Acm)] A Chain with [Cys[10](S-thiol) and Cys[22](Acm)] B Chain. A-Chain peptide (68.8 mg, 26 μmol) was dissolved in 0.1 mM NH₄HCO₃ or 8 M GdHCl at pH 8.5 (6.0 mL) and added to the purified B chain (79.2 mg, 25.4 μmol) in the same buffer (6 mL). The mixture was stirred vigorously at room temperature or 37 °C for each buffer respectively, and reaction was monitored by analytical RP-HPLC. After 30 min (or 24 h if using the GdHCl buffer), the reaction was terminated by the addition of glacial acetic acid and the target product was isolated by preparative RP-HPLC to give 76.7 mg (13.6 μmol, 47.1%). Again, to help improve yields, the peptide may instead be suspended and loaded onto a Sephadex G25 (fine) column for size-exclusion separation using 10% aqueous HOAc as an eluent.

Relaxin-3. The [Cys[24](Acm)] A chain/[Cys[22](Acm)] B chain (76.7 mg, 13.6 μmol) was dissolved in glacial acetic acid (32 mL) and 80 mM HCl and to this was added dropwise 40.7 mL of 20 mM iodine/acetic acid (0.81 mol). After 1 h, the reaction was stopped by the addition of 40.7 mL of 20 mM ascorbic acid. Preparative RP-HPLC, as described above, was then used to isolate and purify the product (9.0 mg, 1.64 μmol, 12.0% yield, 5.7% overall relative to the starting crude B chain). Synthetic H3 relaxin amide was prepared using a similar route in an overall yield of 11.2%.

Characterization. The purity of the synthetic peptides was assessed by capillary zone electrophoresis (capillary length of 50 cm, 10 kV) in 20 mM sodium citrate buffer (pH 4.0), analytical RP-HPLC, and matrix-assisted laser desorption time-of-flight (MALDI−TOF) mass spectrometry using a Bruker Biflex instrument (Bremen, Germany) in the linear mode at 19.5 kV. Peptide quantitation was by amino acid analysis of a 24-h acid hydrolyzate using a GBC instrument (Melbourne, Australia). For tryptic mapping, about 1 μg of peptide was enzymatically digested for 4 h in 10 μL of 10 mM NH₄HCO₃ at 37 °C using a trypsin/substrate ratio of 1:50 (w/w). Prior to mass analysis, 0.5 μL of digest solution was mixed "on target" with 0.5 μL of matrix (saturated

α-cyanocinnamic acid in 30% aqueous acetonitrile) and left to dry.

Production of Mouse Prorelaxin-3. Recombinant mouse prorelaxin-3 was expressed in *Escherichia coli* as a fusion protein containing yeast ubiquitin fused to the N terminus of mouse prorelaxin-3 (*22*). Inclusion bodies containing the ubiquitin−prorelaxin-3 fusion protein were dissolved at ~1 mg/mL in 6 M GdHCl/50 mM Tris-HCl at pH 9.0/1 mM EDTA. After centrifugation (10000*g*, 5 min), the solubilized protein was diluted by the slow addition of 5 volumes of 50 mM Tris-HCl at pH 8.7 containing 1 mM EDTA, 0.05% Tween 80, 0.2 M arginine, 1.25 mM reduced glutathione, and 0.25 mM oxidized glutathione (*23*). A maximal yield of correctly refolded prorelaxin assessed by RP-HPLC on a 250 × 2 mm (i.d.) C4 column (Phenomenex, Torrance, CA) employing a 0.1% TFA/acetonitrile solvent system was achieved after ~2 h of refolding. The solution was subsequently dialyzed against two changes of 50 volumes of 25 mM Tris-HCl at pH 8.0. The dialyzed solution was centrifuged (10000*g*, 15 min) to remove precipitated protein. Cleavage of the ubiquitin moiety was initiated by the addition of 1 part in 30 (w/w) of an *E. coli*-derived recombinant yeast ubiquitin protease-2 (UBP-2) preparation. After 20 h, the reaction mixture containing 25 mg of protein was applied to a 7.5-mL Q-Sepharose Fast Flow column (Amersham Biosciences), equilibrated in 25 mM Tris-HCl at pH 8.2 (buffer A). The protein was eluted with a 0−300 mM NaCl gradient in buffer A over 10 column volumes. Prorelaxin-3-enriched fractions were concentrated by applying ~5 mg onto a 1-mL Waters C18 Sep-Pak cartridge (Milford, MA) equilibrated in 0.1% TFA. The bound prorelaxin-3 was eluted with a single 0.1% TFA/60% acetonitrile wash. The Sep-Pak eluate was diluted 3-fold with 0.1% TFA and applied to a 100 × 10 mm (i.d.) 300 Å Brownlee C4 column (Alltech, Sydney, Australia). The mobile-phase composition was as follows: 0.1% TFA (phase A) and 0.1% TFA/ acetonitrile (phase B). Gradient elution was performed at 25 °C and 5 mL/min from 20 to 60% phase B in 50 min, and the absorbance was monitored at 214 nm. Fractions collected having an HPLC-determined purity >98% were pooled. The protein was formulated by adding equal parts of glycine and mannitol and dried down under vacuum. Purified prorelaxin-3 gave a single band upon reducing and nonreducing SDS−PAGE (results not shown). Mass spectrometry analysis produced a mass of 12 511 Da, in agreement with the predicted mass of oxidized mouse prorelaxin-3. Prorelaxin-3 concentrations were determined by measuring the absorbance at 280 nm using an extinction coefficient of 26 040 M⁻¹ cm⁻¹ (*24*).

Preparation and Measurement of Ubiquitin Protease 2 (UBP-2) Activity. Full-length yeast UBP-2 was expressed in *E. coli* (*25*), and the soluble protein was partially purified by ammonium sulfate precipitation of the cell homogenate (0−45% saturated (NH₄)₂SO₄, 4 °C). Ammonium-sulfate-derived pellets were resuspended in a minimal amount of water and stored in aliquots at −20 °C. *In vitro* UBP-2 activity was measured using purified ubiquitin-human growth hormone fusion protein (ubi-hGH) as the substrate. The reaction mixture containing 2 μL of 0.25 M Tris-HCl at pH 8.0/10 mM EDTA, 14 μL of a 2 mg/mL solution of ubi-hGH, 4 μL of the enzyme preparation, and 4 μL of water was incubated at 30 °C for 30 min. The reaction was stopped

with the addition of 6.7 μL 0.26 M Tris-HCl at pH 6.8/8% SDS/40% glycerol/0.02% bromophenol blue (4× Laemmli SDS-loading buffer). Samples were denatured by heating at 70 °C for 10 min, prior to loading 13.3 μL onto a Novex NuPAGE 4−12% gradient gel as instructed by the supplier (Invitrogen, Carlsbad, CA). Each gel included standards of 2 and 4 μg purified human growth hormone (hGH). Gels were stained with Coomassie blue R-250. UBP-2 activity was assessed by visual comparison of hGH generated in the test samples against the hGH standards.

Circular Dichroism (CD) Spectroscopy. CD spectroscopy was performed using a Jasco J-720 spectropolarimeter and a 0.2 mm path-length cell in the 178−260-nm range. The peptide was dissolved in water (0.5 mg/mL, approximately 80 nM), and spectra were taken in the 180−260-nm wavelength range. Curves were smoothed by an algorithm provided by Jasco. The mean residue ellipticity ($[\theta]_{MR}$) is expressed in degrees cm^2 dmol^{-1} by using a mean residue mass of 110 Da. Because the secondary structures of the peptides provided by the current computer-assisted curve-analyzing algorithms show a high error rate, evaluations of the CD spectra were based on a comparison with known peptide conformations (*26*).

Binding and Signaling Assays. Cells expressing relaxin family peptide receptors were tested for their ability to bind or be activated by H3 relaxin and mouse prorelaxin-3 in comparison to the relevant control peptides, H2 relaxin (recombinant peptide provided by BAS Medical, San Mateo, CA) and H1 relaxin (*27*) for LGR7 and human INSL3 (*28*) for LGR8. Relevant stably transfected cell lines or transiently transfected cells, human LGR7 and LGR8 (*29*), rat and mouse LGR7 (*30*), and rat and mouse LGR8 (*31*) all in HEK293T cells and human GPCR135 in CHO cells (*32*), have been described previously.

Whole-cell-binding assays in 24-well plates using [^{33}P]-labeled H2 relaxin were performed as previously described (*33*). To determine the peptide activity cells were stimulated for 30 min with various concentrations of peptides. LGR7 and LGR8 were tested in parallel with H2 relaxin or human INSL3, respectively (both 100 nM), and GPCR135 with forskolin (5 μM) to determine the maximum cellular cAMP response. cAMP accumulation was measured in cell lysates as previously described (*33*). All data were analyzed using GraphPad PRISM (GraphPad Software, San Diego, CA). A nonlinear regression one-site binding model was used to obtain pK_i (competition binding), whereas sigmoidal dose−response curves were used to calculate pEC$_{50}$. All values are expressed as means ± standard error (SE) of the mean of 3−4 separate observations.

Analysis of In Vitro LGR7 Activity. On the basis of the ability of H2 relaxin to stimulate matrix metalloproteinase-2 (MMP-2) expression by neonatal rat ventricular fibroblasts (*34*), which naturally express the LGR7 receptor, the synthetic H3 relaxin peptide was assayed for relaxin-like activity *in vitro*, using these cells. Briefly, fibroblasts (1 × 10^5 cells/per well; 12-well plate) were either treated with 1, 10, or 100 ng/mL H3 relaxin or 100 ng/mL H2 relaxin, in the absence or presence of transforming growth factor β (TGF-β; 2 ng/mL) for 72 h, with the final 24 h of treatment being under serum-free conditions. Four separate experiments were conducted in duplicate, while untreated cultures were used as controls. Equal aliquots of the collected media were

then analyzed by gelatin zymography, as described previously (*34*). For quantitation of MMP-2 expression, samples were diluted 20-fold, before being analyzed by gelatin zymography (to avoid saturation of the MMP-2 bands). Densitometry of the latent (L) and active (A) MMP-2 bands was performed using a BioRad GS-710 Calibrated Imaging Densitometer (Richmond, CA) and Quantity-One software (BioRad). pEC$_{50}$ values were calculated as described for cAMP accumulation assays.

In Vivo Bioassay: Water Drinking in Rats. The synthetic H3 relaxin peptide was assayed for relaxin-like activity *in vivo* using an established model of water drinking in rats (*35*). Male Sprague Dawley rats (280−300 g; $n = 3-4$ per group) were housed in individual cages with *ad libitum* access to pelleted food and water. Procedures were approved by the HFI Animal Welfare Committee, in compliance with the guidelines of the National Health and Medical Research Council of Australia. Rats were anaesthetized with sodium pentobarbital (50 mg/kg, i.p.) and positioned in a stereotaxic frame (Kopf Instruments, Tujunga, CA). Stainless steel cannulae (7 mm, 23 gauge) were implanted into the lateral ventricle [coordinates: anteroposterior, −0.2 mm from bregma; mediolateral, −1.5 mm from midline; dorsoventral, −4.0 mm from the skull surface] according to the atlas of Paxinos and Watson (*36*). Cannulae were affixed to the skull with surgical screws and dental cement. Rats were allowed to recover for 7 days. Prior to treatment, water drinking was measured every 15 min for 45 min. Injections were then made using a 5-μL Hamilton microsyringe connected to the cannula with polyethylene tubing. A 1-μL volume of H2 or H3 relaxin (50 or 150 ng in 1 μL of aCSF, respectively) was infused over 20 s (control untreated rats received no infusion), after which rats were returned to their cages and water intake was monitored every 15 min for a further 90 min. *In situ* hybridization histochemistry and [^{33}P]-H2 relaxin-binding autoradiography were performed as previously described (*18, 37*).

RESULTS

The individual A- and B-chain peptides were subjected to continuous flow Fmoc-solid-phase synthesis in which pairs of cysteines were selectively *S*-thiol-protected with masking groups that allowed their individual removal and subsequent stepwise disulfide-bond formation. The intramolecular disulfide bond within the A chain was formed by oxidation of the two free *S*-thiols with DPDS after which the *S-tert*-butyl protecting group on cysteine 11 of the A chain was converted to the *S*-pyridinyl by treatment of the peptide with DPDS in the presence of TFMSA. The resulting A chain was then in a form suitable for direct combination with the corresponding B chain via thiolysis. Final intermolecular disulfide-bond formation was achieved by iodinolysis of the *S*-Acm groups on each of the two chains. The overall yield of synthetic H3 relaxin was 5.7% relative to the starting B chain. Curiously, yields were significantly higher (11%) when H3 relaxin was prepared in which the C-terminal of the A and B chains were in the amide form. Comprehensive chemical characterization including by analytical RP-HPLC (Figure 3) and MALDI−TOF MS (theory, MH+ 5500.5; found, MH+ 5499.6) confirmed the high purity of the synthetic products. Tryptic mapping of an aliquot produced the expected pattern of fragments that was identified by subsequent MALDI−TOF
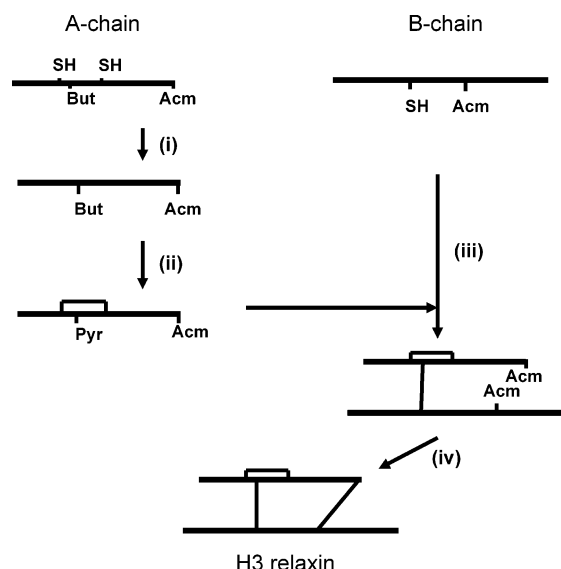
FIGURE 2: Scheme for regioselective disulfide-bond formation of human relaxin-3 following solid-phase synthesis of individual A and B chains. (i) Aqueous DPDS, pH 8.5; (ii) DPDS/TFMSA/TFA; (iii) thiolysis at pH 8.0; and (iv) iodine/aqueous HOAc. Abbreviations: Acm, acetamidomethyl; Bu*t*, *tert*-butyl; Pyr; 2-pyridine-sulfenyl.
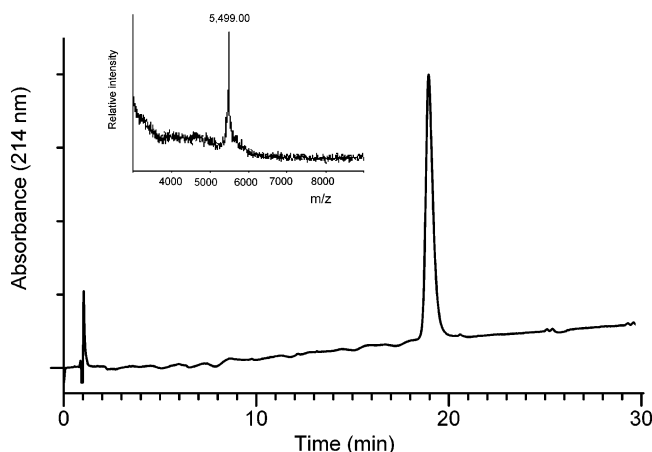

FIGURE 3: Analytical RP-HPLC of synthetic human relaxin-3. Column, Vydac C18 (4.6 mm i.d. × 250 mm); gradient, 20−50% B over 30 min. Eluent A, 0.1% aqueous TFA; eluent B, 0.1% TFA/CH_3CN. (Inset) MALDI−TOF mass spectrum of purified synthetic human relaxin-3. Calculated MH+, 5499.4; found MH+, 5499.0 Da.

MS and confirmed the parallel alignment of the A and B chains and the cystine cross-links (data not shown).

The synthetic H3 relaxin peptide amide in water exhibited a CD spectrum typical for repeated β turns and loosened (3_{10}) helices. The spectrum was characterized by a positive band at 188 nm, a negative band at 206 nm, and a negative shoulder at 222 nm (Figure 4). A comparison of the spectral features with those of H2 relaxin clearly showed the synthetic H3 relaxin to possess a less developed α-helix structure. The H2 relaxin product appeared to be more α-helical as documented by (i) a red shift of both $\pi\pi*$ bands; (ii) an increased 222:208 (206) nm band ratio; and (iii) a decreased sensitivity of the spectra to organic cosolvents or additives known to stabilize helical structures. Indeed, when the spectra were collected in aqueous trifluoroethanol (TFE) solutions, little changes were observed for H2 relaxin, as opposed to

major structural alterations found for the H3 relaxin variant. For the latter peptide, the addition of 10% TFE or 2% octyl-β-D-glucoside resulted in a significantly increased helical potential as reflected by a red shift of the bands to 190−192 and 207−208 nm, an increase of band intensities, and the 222:208 nm band ratio (Figure 4). Interestingly, the addition of phosphate-buffered saline also increased the helix propensity, an effect that is likely due to stabilization of intrahelical salt bridges between positive and negative charges three or four residues apart along the helix barrel.

The ability of the synthetic H3 relaxin peptide to activate relaxin family peptide receptors was tested for the first time in comparison to a relaxin-3 prohormone, H1 relaxin, and native ligands. Furthermore, the activities on LGR7 and LGR8 receptors from human, mouse, and rat were compared. Importantly, the amide form of H3 relaxin was used throughout because it demonstrated identical cAMP activity to the acid form at both GPCR135 (amide pEC_{50} = 9.25 ± 0.09; acid pEC_{50} = 9.3 ± 0.08) and LGR7 (amide pEC_{50} = 8.19 ± 0.08; acid pEC_{50} = 8.08 ± 0.08). Results of binding to human LGR7 and LGR8 and cAMP accumulation results for all LGR7 and LGR8 receptors are shown in Figure 5. Additionally, pooled pEC_{50} and pK_i results are outlined in Table 1. Importantly, binding affinities to human LGR7 closely matched the activities of each peptide to induce cAMP accumulation. The rank order of potency of human relaxin peptides at human LGR7 was H2 > H1 > H3 relaxin. The affinity of H3 relaxin for rat and mouse LGR7 was very similar to its affinity for human LGR7 and hence also demonstrated an approximately 50-fold lower affinity for these receptors than H2 relaxin. The binding affinity of mouse prorelaxin-3 for both human and mouse LGR7 (human, pK_i = 8.00 ± 0.087; mouse, pK_i = 7.62 ± 0.23) was slightly lower than H3 relaxin peptide (pK_i = 8.50 ± 0.11; pK_i = 8.26 ± 0.075), although this difference was only significant for human LGR7 (p < 0.05; unpaired t test). Both H3 relaxin and mouse prorelaxin-3 were unable to stimulate cAMP accumulation in human LGR8-expressing cells at concentrations up to 1 μM, although H3 relaxin will bind to human LGR8 with low affinity (pK_i = 6.97 ± 0.09). However, interestingly, H3 relaxin was able to bind and activate rat and mouse LGR8, although its activity (mouse LGR8, pEC_{50} = 6.65 ± 0.05; rat LGR8, pEC_{50} = 6.69 ± 0.12) was slightly lower than its affinity for the receptors (mouse LGR8, pK_i = 7.23 ± 0.14; rat LGR8, pK_i = 7.49 ± 0.19). H3 relaxin was able to activate human GPCR135 with high efficacy (pEC_{50} = 9.25 ± 0.09) (Table 1).

The biological activity of synthetic H3 relaxin was also tested in a previously characterized primary fibroblast culture model, which was shown to naturally express LGR7. The administration of H3 relaxin alone to rat ventricular fibroblasts induced a significant, dose-dependent increase in MMP-2 expression at concentrations of 1 ng/mL (by 22.6%, p < 0.05), 10 ng/mL (by 39.5%, p < 0.01), and 100 ng/mL (by 50.6%, p < 0.01) over 72 h, as compared to MMP-2 levels detected in untreated cultures (Figure 6). H2 relaxin treatment (100 ng/mL) induced a 62.2% (p < 0.01) increase in MMP-2 expression over the same time period (Figure 6). In separate experiments, TGF-β (2 ng/mL) alone induced a 20.4% (p < 0.05) increase in MMP-2 expression over 72 h, compared to that observed in untreated cultures (Figure 6). The administration of synthetic H3 to TGF-β-stimulated cells
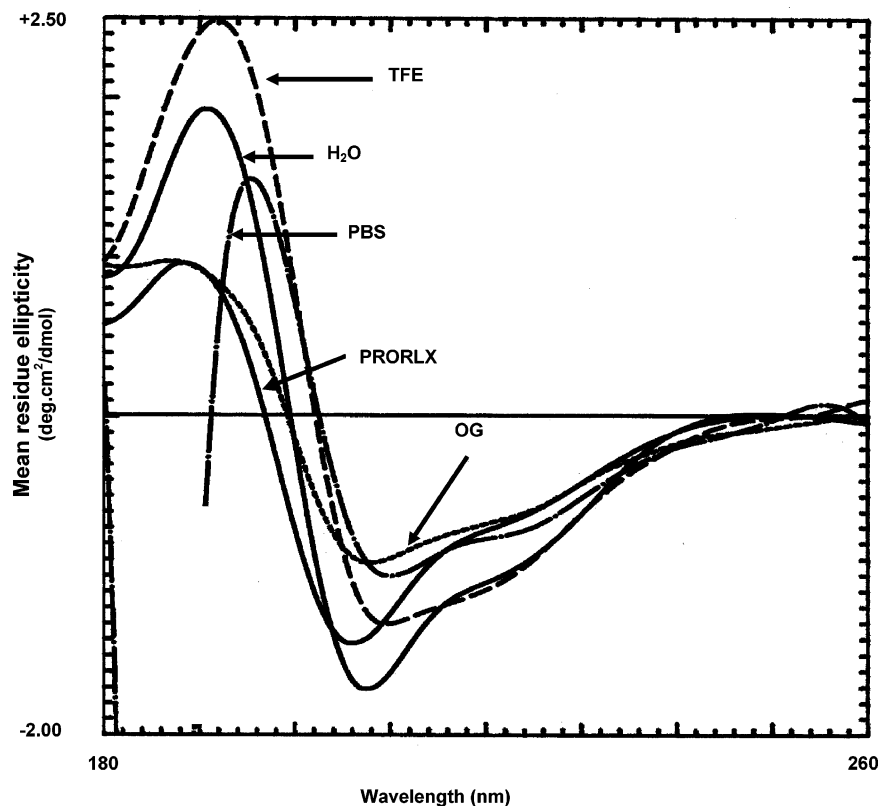
FIGURE 4: CD spectra of synthetic H3 relaxin recorded in water (—), PBS (-·-), 2% aqueous octyl-β-D-glucoside (OG) (- - -), and 50% aqueous TFE (− −) solutions. The spectrum of recombinant DNA-derived mouse prorelaxin-3 is also shown for a comparison.

further increased MMP-2 expression at concentrations of 1 ng/mL (by 21.3%, $p < 0.01$), 10 ng/mL (by 36.9%; $p < 0.01$), and 100 ng/mL (by 48.7%; $p < 0.01$), compared to MMP-2 levels stimulated by TGF-β alone (Figure 6). Again, the maximal effect of H3 relaxin was similar to that of H2 relaxin, which induced a 59.8% increase in MMP-2 expression ($p < 0.01$) in the presence of TGF-β over a 72-h period (Figure 6). The efficacy of the H3 relaxin effect was extremely potent and was similar in the absence ($pEC_{50} = 9.43 \pm 0.12$) or presence of TGF-β ($pEC_{50} = 9.64 \pm 0.48$).

The biological activity of synthetic H3 relaxin was tested in a previously established *in vivo* model of relaxin activity, the induction of water drinking in rats following central infusion. The effect of relaxin on drinking following both peripheral and central administration is thought to be via relaxin receptors in the subfornical organ (SFO). High levels of both LGR7 mRNA and relaxin binding sites are present in the rat SFO (Figure 7A, A′), consistent with previous results from our laboratory (*18, 37*). In the current studies, groups of rats received infusion of H2 relaxin (50 ng) or H3 relaxin (50 and 150 ng) into the lateral ventricle and water drinking was measured every 15 min thereafter (Figure 7B). Within 15 min of treatment, rats treated with H2 or H3 relaxin were drinking significantly greater volumes compared to untreated rats ($p < 0.05$). Comparatively, the 50 ng of H2 relaxin dose stimulated a greater drinking response than the equivalent dose of H3 relaxin. This finding agrees with their corresponding *in vitro* activity at LGR7 (see above). A 3-fold higher dose of H3 relaxin (150 ng) stimulated a greater drinking response than that of 50 ng of H2 relaxin or H3 relaxin.

DISCUSSION

The discovery of a third human relaxin gene during a search of the genomic databases was both unexpected and exciting and raises many questions regarding the evolution and biological roles of not only the three individual relaxins but also the nature of the interplay between these peptides *in vivo*. Significant homology differences exist between the relaxins, although each possesses what is now recognized to be a characteristic relaxin fingerprint, a receptor binding region within the B chain and consisting of the sequence Arg-X-X-X-Arg-X-X-Ile/Val (*2*). In contrast to the primary structures between species of relaxins 1 and 2 that show significant heterogeneity, relaxin-3 sequences from human to fugu and zebrafish show a very high degree of evolutionary conservation in their A and B chains (*2*). The connecting C peptides of the H1 and H2 relaxin are extraordinarily long, being approximately 105 residues in length, whereas that of H3 relaxin is about 66 residues. Detailed phylogenetic analysis strongly suggests that the *RLN3* gene is in fact the precursor to the entire relaxin peptide family (*2*).

Relaxin acts via a G-protein-coupled receptor known as LGR7. It is characterized by the presence of a large ectodomain containing leucine-rich repeats. Recent studies have identified two binding sites on LGR7, one primary site within the ectodomain and a secondary site on the transmembrane extracellular loops (*12, 29*). Further, the interaction between the two sites is critical for ligand-directed signal transduction (*12, 29*). In contrast, the relaxin-3 receptor was recently identified as being closely related to the receptors for somatostatin and angiotensin and is marked by the absence of a significant extracellular domain (*5*). Thus, it is likely that relaxin-3 initiates its biological effect via interac-
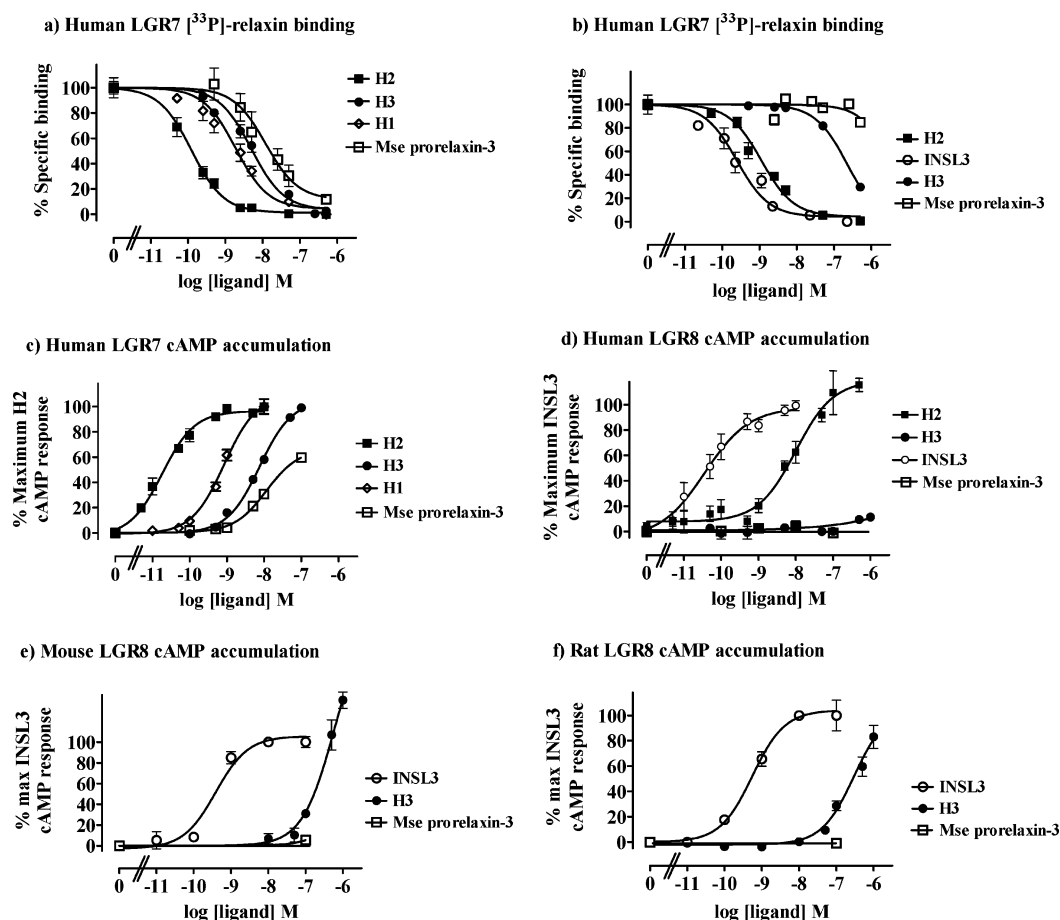
FIGURE 5: Competition binding and cAMP accumulation response of cells transfected with various LGR7 and LGR8 receptors in response to H3 relaxin and other relaxin family peptides. Whole-cell [^{33}P]-H2 relaxin competition binding expressed as the percentage of specific binding in human LGR7 (a) and LGR8 (b) transfected 293T cells. cAMP accumulation expressed as the percentage of the maximum H2 relaxin or INSL3 response in human LGR7 (c), human LGR8 (d), mouse LGR8 (e), and rat LGR8 (f) transfected 293T cells. H2, recombinant human gene-2 relaxin; H3, synthetic H3 relaxin; H1, synthetic H1 relaxin; INSL3, synthetic human INSL3; Mse prorelaxin-3, recombinant mouse prorelaxin-3.

Table 1: Pooled Binding (pK_i) and cAMP Accumulation (pEC_{50}) Data of Various Relaxin Family Peptide Receptors with Relaxin Family Peptides[a]

		H3 relaxin			H2 relaxin				INSL3				mouse prorelaxin-3			H1 relaxin		
		mean	SEM	n =	mean	SEM	n =		mean	SEM	n =		mean	SEM	n =	mean	SEM	n =
human LGR7	pEC_{50}	8.19	0.078	3	10.6	0.044	4		5.4	1.025	2		7.96	0	1	9.1	0.11	3
	pK_i	8.5	0.11	3	10.21	0.36	3	b	5.97	0.14	3		8	0.087	3	8.84	0.17	3
mouse LGR7	pEC_{50}	ND[c]			9.89	0.039	3	d	>5		3		NA[e]		1	ND[c]		
	pK_i	8.26	0.075	3	f	9.88	0.023	3	d	>5		3		7.62	0.23	3	ND[c]		
rat LGR7	pEC_{50}	ND[c]			9.6	0.065	3	d	>5		3		NA[e]		1	ND[c]		
	pK_i	8.38	0.05	3	f	9.63	0.058	3	d	>5		3		ND[c]			ND[c]		
human LGR8	pEC_{50}	>5		3	7.94	0.085	3		9.4	0.089	3		NA[e]		1	ND[c]		
	pK_i	6.97	0.091	3	9.27	0.19	4	b	9.66	0.17	3		>5		3	8.83	0.28	3
mouse LGR8	pEC_{50}	6.65	0.054	3	ND[c]				9.37	0.039	3		ND[c]			ND[c]		
	pK_i	7.23	0.14	2	8.38	0.2	3		8.72	0.13	3		ND[c]			ND[c]		
rat LGR8	pEC_{50}	6.69	0.12	3	ND[c]				9.25	0.065	3		ND[c]			ND[c]		
	pK_i	7.49	0.19	3	g	8.55	0.1	3	g	8.99	0.18	3	g	ND[c]			ND[c]		
human GPCR135	pEC_{50}	9.25	0.092	3	NA[e]				NA[e]				ND[c]			ND[c]		
	pK_i	ND[c]			NA[e]				NA[e]				ND[c]			ND[c]		

[a] Data are mean ± SEM of 3−4 experiments. Peptides were tested in triplicate in individual experiments. [b] From ref *29*. [c] ND, not determined. [d] From ref *30*. [e] NA, no activity. [f] From ref *54*. [g] From ref *31*.

tions with the transmembrane domains and extracellular loops in a fashion similar to other peptide receptors of this type.

The predicted primary structure of H3 relaxin is shown in Figure 1 and consists of a 24-residue A chain linked to a 27-residue B chain via characteristic insulin cystine cross-links. Curiously, original attempts in our laboratory to produce the hormone by conventional combination of the individual synthetic A and B chains did not meet with success. This is in contrast to the successful acquisition of insulin and H2 relaxin by this approach (*38, 39*). Recent work on the folding and combination of H2 relaxin suggested that it follows a pathway similar to that of insulin in which the N-terminal α helix of the A chain is an initiation site for subsequent folding (*40*). Secondary-structure predictions for
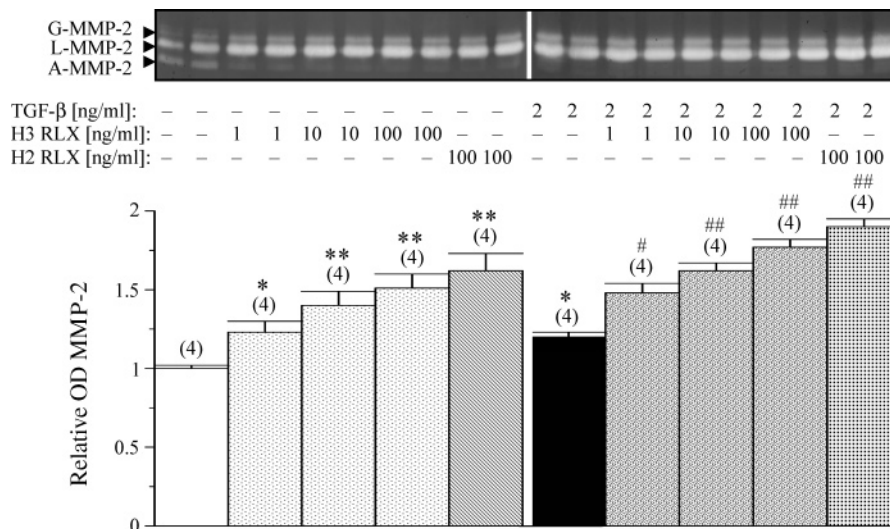
FIGURE 6: MMP-2 expression and activity were determined by gelatin zymography of media from untreated cultures and cell treated with either H3 relaxin (1, 10, and 100 ng/mL) or H2 relaxin (100 ng/mL) alone (upper left panel). In separate experiments, media from cultures treated with TGF-β (2 ng/mL) alone or in the presence of H3 relaxin (1, 10, and 100 ng/mL) or H2 relaxin (100 ng/mL) was also analyzed (upper right panel). Shown are the glycosylated (G), latent (L), and active (A) forms of MMP-2, from a representative zymograph of duplicate samples from each group, from four separate experiments conducted in the absence or presence of TGF-β. Also shown are the mean $\pm$ SE relative OD MMP-2 of the total MMP-2 (derived from the latent and active forms of MMP-2), as determined by densitometry scanning. For quantitative analysis, all samples were diluted by a factor of 1 in 20 to ensure that the MMP-2 bands were not saturated. (*) $p < 0.05$ and (**) $p < 0.01$ versus relative values from untreated cultures; (#) $p < 0.05$ and (##) $p < 0.01$ versus relative values from TGF-β alone treated cultures.
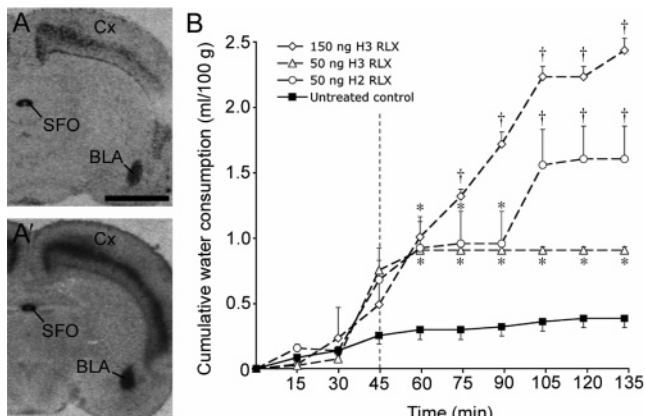

FIGURE 7: Distribution of LGR7 mRNA (A) and [^{33}P]-H2 relaxin binding sites (A′) in coronal sections of rat forebrain at the level of the subfornical organ. Effect of relaxin-2 (50 ng) and relaxin-3 (50 and 150 ng) infusions into the lateral ventricle on drinking responses in rats (B). Cumulative water consumption (mean SEM; $n = 3-4$ rats per group) was measured every 15 min for 30 min prior to infusions and 105 min following infusions. (*) $p < 0.05$ and (†) $p < 0.001$ as compared to the untreated group (one-way ANOVA, Bonferroni post hoc test). Abbreviations: BLA, basolateral amygdala; Cx, cerebral cortex; SFO, subfornical organ. Scale bar = 2.5 mm.

H3 relaxin show that, unlike H1 and H2 relaxins, the N terminus of the A chain of H3 relaxin is likely to adopt a predominant random coil because of the presence of three successive serine residues. This is supported by the CD spectrum of the peptide that showed a smaller degree of α helix than for H2 relaxin. The absence of this helical propensity and thus combination initiation site clearly suggests that folding of the propeptide must follow an alternative route to that proposed for insulin and the insulin-like growth factor. Thus, an alternative strategy was devised and adopted for the preparation of the H3 relaxin, that of regioselective disulfide-bond synthesis, which has been used

in various forms for a number of insulin-like peptides including H2 relaxin, insulin, and bombyxin (*21, 41−43*).

Initial attempts to prepare H3 relaxin using the cysteine *S*-thiol protecting group permutation employed for the regioselective synthesis of insulin (*42*) met with little success. Displacement of a pair of *S-tert*-butyl groups and simultaneous disulfide-bond formation with a combination of phenyl sulfoxide and trimethylchlorosilane caused substantial destruction of a pair of tryptophan residues within each of the A and B chains in a known side reaction. This amino acid is absent within the insulin molecule. Further small-scale assemblies led to the eventual adoption of a strategy of use of judiciously placed *S*-trityl, *S-tert*-butyl, and *S*-Acm protecting groups (Figure 2). The formation of the first, intramolecular disulfide bond within the A chain was achieved by oxidation with DPDS′ (*44*). The resulting peptide was then subjected to conversion of the *S*-Bu^t function to *S*-pyridinyl, followed by combination in solution with the corresponding S-protected B chain, in which the two intermolecular disulfide bonds were formed sequentially by thiolysis and iodolysis. The latter reaction was carried out under tightly controlled conditions to minimize the modification of the two tryptophan residues in each of the A and B chains of the peptide. The placement of the *S*-Acm groups and thus order of disulfide-bond formation was critical for the success of the synthesis of the peptide. Originally, the *S*-Acm group was placed in cysteines 11 and 10 of the A and B chains, respectively (*7*). Subsequent iodolysis of the penultimate relaxin intermediate led to a substantial loss of peptide because of the predominant modification of the nearby tryptophan 13 in the A chain (data not shown). Placement of the *S*-Acm groups further away from this residue at cysteines 24 and 22 of the A and B chains resulted in dramatically improved yields of the final product. Final purification by RP-HPLC yielded the synthetic H3 relaxin in a good overall yield of about 6% relative to the starting

B-chain peptide compared to the previously reported 0.7% (7). Curiously, still better overall yields (11%) were obtained using C-terminal amides of the A and B chains. Importantly, the quantities of synthetic relaxin-3 obtained by the solid-phase approach far exceeds what has been achieved previously. Furthermore, this yield was far greater than that achieved through the considerable effort of preparing mouse prorelaxin-3 recombinantly, which only produced 250 μg of purified protein. This is further complicated by the need for subsequent *ex vivo* excision of the connecting C peptide in the recombinant material to mimic the native peptide.

Comprehensive chemical characterization of synthetic H3 relaxin by analytical RP-HPLC and MALDI−TOF mass spectrometry demonstrated the high integrity of the synthetic product (Figure 3). Tryptic mapping followed by MS analysis further confirmed the disposition of the disulfide bonds (results not shown). Secondary-structural analysis by CD spectroscopy showed it to adopt a less ordered conformation than H2 relaxin, reflecting the presence in the former of a greater percentage of non-α-helical forming amino acids. There was no significant structural difference between the C-terminal acid and amide forms of the peptide (data not shown).

The synthetic H3 relaxin peptide was tested in parallel to mouse prorelaxin-3 for its ability to bind and activate the LGR7 and LGR8 receptors from human, rat, and mouse and human GPCR153. Although the rank order of potency of human relaxin peptides at human LGR7 was H2 > H1 > H3 relaxin, the activity of H3 relaxin was still in the low nanomolar range. Importantly, H3 relaxin showed similar activity on all of the LGR7 receptors, indicating that it is likely a ligand for LGR7 in all of these species. This has important implications for the biology of relaxin-3, especially in the brain (see below). Surprisingly, in the same assays, mouse prorelaxin-3 was found to show similar activity to H3 relaxin, suggesting that the removal of the 66-residue C peptide was not a strict requirement for biological activity. The core structure of the prorelaxin presumably retains a significant native structure for the presentation of the active site to its receptor. Unexpectedly, H3 relaxin was shown to activate rat and mouse LGR8, whereas it is unable to stimulate human LGR8 at concentrations up to 1 μM. The concentrations of H3 relaxin required to activate mouse and rat LGR8 (high nanomolar) are quite high, hence it remains to be seen if this has any relevance *in vivo*. However, it does demonstrate that any analogues or mimetics of relaxin-3 should be carefully tested for their activities on LGR8 and testing in rodent models should take into account the possibility of activating LGR8 at high concentrations. Importantly, the synthetic H3 relaxin showed a very similar efficacy at human GPCR135 to that reported previously with recombinant H3 relaxin (5).

Synthetic H3 relaxin was also able to stimulate native LGR7 receptors *in vitro*. When applied to neonatal rat ventricular fibroblasts, which express LGR7 (34) and not GPCR135 (data not shown), it stimulated an increase in the MMP-2 expression in a dose-dependent manner. Importantly, H3 relaxin was extremely potent (EC$_{50}$ ∼ 0.3 nM) at inducing this effect and demonstrated a similar maximum response as H2 relaxin. Furthermore, H3 relaxin was also able to stimulate MMP-2 expression in the presence of the profibrogenic factor, TGF-β (45). This effect was almost equivalent

to the maximal H2 relaxin response, and the potency of this effect was very similar to that demonstrated in the absence of TGF-β. Importantly, both of these results indicate that H3 relaxin demonstrates a higher activity at the native rat LGR7 receptor than at the recombinant receptor expressed in HEK-293T cells.

MMP-2 has been shown to cleave type-I collagen (46) and other extracellular matrix (ECM) components (such as fibronectin and nonfibrillar collagens), known to be upregulated during fibrosis (organ scarring). Hence, it is possible that the deposition of the interstitial collagens and other ECM molecules can be influenced by H3 relaxin via its ability to stimulate MMP-2 expression and/or activation. Importantly, these findings demonstrate that H3 relaxin is able to induce its effect on MMP-2 (and potentially other ECM components) via LGR7 in a fashion similar to H2 relaxin. However, it should be noted that the physiological significance of relaxin-3 as an antifibrotic agent is still being established. Relaxin knockout mice, which lack a functionally active *RLN1* gene (47), develop an age-related progression of fibrosis in several organs (48−50), despite these tissues expressing relaxin-3 mRNA. In the lung of relaxin knockout mice (49), no significant differences in relaxin-3 mRNA expression were detected with age, suggesting that relaxin-3 does not play a direct role *in vivo* or is not as influential as relaxin in regulating the progression of fibrosis. Nevertheless, our findings in this study demonstrate that relaxin-3 is able to mimic some of the actions of relaxin via the activation of LGR7 and may also regulate a number of ECM components via similar mechanisms. Importantly, during the preparation of this paper, a study was published indicating that relaxin-3 can reverse cardiac fibrosis *in vivo* (51).

Synthetic H3 relaxin also stimulated water drinking following central infusion in rats. The relative potency of H3 versus H2 relaxin suggests that H3 relaxin has a slightly lower activity at LGR7, consistent with the *in vitro* data. The effects on water drinking are consistent with an action on the LGR7 receptor in the subfornical organ, demonstrated in this study and previously (18, 19). This distribution of LGR7 receptors is identical to the pattern of activation produced by relaxin infusion (35). There is currently no evidence for actions of relaxin-3 at GPCR135 in the circumventricular organs such as the SFO or reports of GPCR135 expression in these regions. Hence, these studies demonstrate that H3 relaxin can activate LGR7 *in vivo*. Further roles for relaxin-3 have emerged in recent studies that demonstrated both intracerebroventricular and intraparaventricular nucleus (iPVN) injections of H3 relaxin (obtained from a commercial supplier) to satiated rats significantly increased food intake 1 h post-administration in the early light phase and the early dark phase (10). In contrast, equimolar doses of H2 relaxin, which preferentially binds LGR7 and not GPCR135, did not increase feeding. These results suggest a role for relaxin-3 in appetite regulation via actions within the hypothalamic feeding circuits, possibly via actions at GPCR135. In morphological examinations, relaxin-3 mRNA and peptide immunoreactivity was found to be highly expressed in neurons of the NI in the median dorsal tegmental pons of the rat (6) and mouse (7) and relaxin-3 containing nerve fibers were found broadly distributed within the forebrain (9). Levels of relaxin-3 mRNA increased significantly in the NI after prolonged water

immersion and restraint stress, leading to the suggestion that relaxin-3-containing neurons in the NI that express high levels of receptors for the stress hormone corticotropin-releasing factor (CRF) (*52*) are involved in the regulation of the stress response (*9, 53*).

In summary, this study describes an efficient methodology for the synthesis of significant quantities of H3 relaxin, which will allow further systematic studies to more clearly define the neurological function of relaxin-3. Indeed, the availability of this peptide has allowed a recent determination of its solution structure by NMR spectroscopy (*55*). Further, this work clearly demonstrates that relaxin-3 will bind and activate LGR7, the relaxin receptor, at physiological concentrations, both *in vitro* and *in vivo*. It is therefore likely that relaxin-3 is another natural ligand of LGR7 and that there is a complex interaction of relaxin peptides and relaxin peptide receptors in the brain. Further studies are currently underway to provide a resolution to and understanding of this fascinating relationship.

ACKNOWLEDGMENT

REFERENCES

1. Hsu, S. Y. (2003) New insights into the evolution of the relaxin-LGR signaling system, *Trends Endocrinol. Metab. 14*, 303−309.
2. Wilkinson, T. N., Speed, T. P., Tregear, G. W., and Bathgate, R. A. D. (2005) Evolution of the relaxin-like peptide family, *BMC Evol. Biol. 5*, 14.
3. Bathgate, R. A., Samuel, C. S., Burazin, T. C., Gundlach, A. L., and Tregear, G. W. (2003) Relaxin: New peptides, receptors, and novel actions, *Trends Endocrinol. Metab. 14*, 207−213.
4. Bathgate, R. A. D., Hsueh, A. J., and Sherwood, O. D. (2005) Physiology and molecular biology of the relaxin peptide family, in *Physiology of Reproduction* (Knobil, E., and Neill, J. D., Eds.) in press, Elsevier, San Diego, CA.
5. Liu, C., Eriste, E., Sutton, S., Chen, J., Roland, B., Kuei, C., Farmer, N., Jornvall, H., Sillard, R., and Lovenberg, T. W. (2003) Identification of relaxin-3/INSL7 as an endogenous ligand for the orphan G-protein-coupled receptor GPCR135, *J. Biol. Chem. 278*, 50754−50764.
6. Burazin, T. C., Bathgate, R. A., Macris, M., Layfield, S., Gundlach, A. L., and Tregear, G. W. (2002) Restricted, but abundant, expression of the novel rat gene-3 (R3) relaxin in the dorsal tegmental region of brain, *J. Neurochem. 82*, 1553−1557.
7. Bathgate, R. A., Samuel, C. S., Burazin, T. C., Layfield, S., Claasz, A. A., Reytomas, I. G., Dawson, N. F., Zhao, C., Bond, C., Summers, R. J., Parry, L. J., Wade, J. D., and Tregear, G. W. (2002) Human relaxin gene 3 (H3) and the equivalent mouse relaxin (M3) gene. Novel members of the relaxin peptide family, *J. Biol. Chem. 277*, 1148−1157.
8. Bathgate, R. A. D., Scott, D., Chung, S., Ellyard, D., Garreffa, A., and Tregear, G. W. (2002) Searching the human genome database for novel relaxin-like peptides, *Lett. Pept. Sci. 8*, 129−132.
9. Tanaka, M., Iijima, N., Miyamoto, Y., Fukusumi, S., Itoh, Y., Ozawa, H., and Ibata, Y. (2005) Neurons expressing relaxin 3/INSL 7 in the nucleus incertus respond to stress, *Eur. J. Neurosci. 21*, 1659−1670.
10. McGowan, B. M., Stanley, S. A., Smith, K. L., White, N. E., Connolly, M. M., Thompson, E. L., Gardiner, J. V., Murphy, K. G., Ghatei, M. A., and Bloom, S. R. (2005) Central relaxin-3 administration causes hyperphagia in male Wistar rats, *Endocrinology 146*, 3295−3300.
11. de Meyts, P., and Whittaker, J. (2002) Structural biology of insulin and IGF1 receptors: Implications for drug design, *Nat. Rev. Drug Discovery 1*, 769−783.
12. Bathgate, R. A., Ivell, R., Sanborn, B. M., Sherwood, O. D., and Summers, R. J. (2005) Receptors for relaxin family peptides, *Ann. N. Y. Acad. Sci. 1041*, 61−76.
13. Hsu, S. Y., Nakabayashi, K., Nishi, S., Kumagai, J., Kudo, M., Sherwood, O. D., and Hsueh, A. J. (2002) Activation of orphan receptors by the hormone relaxin, *Science 295*, 671−674.
14. Kumagai, J., Hsu, S. Y., Matsumi, H., Roh, J. S., Fu, P., Wade, J. D., Bathgate, R. A., and Hsueh, A. J. (2002) INSL3/Leydig insulin-like peptide activates the LGR8 receptor important in testis descent, *J. Biol. Chem. 277*, 31283−31286.
15. Liu, C., Chen, J., Sutton, S., Roland, B., Kuei, C., Farmer, N., Sillard, R., and Lovenberg, T. W. (2003) Identification of relaxin-3/INSL7 as a ligand for GPCR142, *J. Biol. Chem. 278*, 50765−50770.
16. Liu, C., Kuei, C., Sutton, S., Chen, J., Bonaventure, P., Wu, J., Nepomuceno, D., Wilkinson, T., Bathgate, R., Eriste, E., Sillard, R., and Lovenberg, T. W. (2005) INSL5 is a high affinity specific agonist for GPCR142 (GPR100), *J. Biol. Chem. 280*, 292−300.
17. Sutton, S. W., Bonaventure, P., Kuei, C., Roland, B., Chen, J., Nepomuceno, D., Lovenberg, T. W., and Liu, C. (2004) Distribution of G-protein-coupled receptor (GPCR)135 binding sites and receptor mRNA in the rat brain suggests a role for relaxin-3 in neuroendocrine and sensory processing, *Neuroendocrinology 80*, 298−307.
18. Burazin, T. C., Johnson, K. J., Ma, S., Bathgate, R. A., Tregear, G. W., and Gundlach, A. L. (2005) Localization of LGR7 (relaxin receptor) mRNA and protein in rat forebrain: Correlation with relaxin binding site distribution, *Ann. N. Y. Acad. Sci. 1041*, 205−210.
19. Piccenna, L., Shen, P. J., Ma, S., Burazin, T. C., Gossen, J. A., Mosselman, S., Bathgate, R. A., and Gundlach, A. L. (2005) Localization of LGR7 gene expression in adult mouse brain using LGR7 knock-out/LacZ knock-in mice: Correlation with LGR7 mRNA distribution, *Ann. N. Y. Acad. Sci. 1041*, 197−204.
20. Bullesbach, E. E., and Schwabe, C. (2000) The relaxin receptor-binding site geometry suggests a novel gripping mode of interaction, *J. Biol. Chem. 275*, 35276−35280.
21. Lin, F., Otvos, L., Jr., Kumagai, J., Tregear, G. W., Bathgate, R. A., and Wade, J. D. (2004) Synthetic human insulin 4 does not activate the G-protein-coupled receptors LGR7 or LGR8, *J. Pept. Sci. 10*, 257−264.
22. Butt, T. R., Jonnalagadda, S., Monia, B. P., Sternberg, E. J., Marsh, J. A., Stadel, J. M., Ecker, D. J., and Crooke, S. T. (1989) Ubiquitin fusion augments the yield of cloned gene products in *Escherichia coli*, *Proc. Natl. Acad. Sci. U.S.A. 86*, 2540−2544.
23. Armstrong, N., de Lencastre, A., and Gouaux, E. (1999) A new protein folding screen: Application to the ligand binding domains of a glutamate and kainate receptor and to lysozyme and carbonic anhydrase, *Protein Sci. 8*, 1475−1483.
24. Gill, S. C., and von Hippel, P. H. (1989) Calculation of protein extinction coefficients from amino acid sequence data, *Anal. Biochem. 182*, 319−326.
25. Baker, R. T., Tobias, J. W., and Varshavsky, A. (1992) Ubiquitin-specific proteases of *Saccharomyces cerevisiae*. Cloning of UBP2 and UBP3, and functional analysis of the UBP gene family, *J. Biol. Chem. 267*, 23364−23375.
26. Perczel, A., Hollosi, M., Sandor, P., and Fasman, G. D. (1993) The evaluation of type I and type II *β*-turn mixtures. Circular dichroism, NMR, and molecular dynamics studies, *Int. J. Pept. Protein Res. 41*, 223−236.
27. Wade, J. D., Lin, F., Salvatore, D., Otvos, L., Jr., and Tregear, G. W. (1996) Synthesis and characterization of human gene 1 relaxin peptides, *Biomed. Pept. Proteins Nucleic Acids 2*, 27−32.
28. Fu, P., Layfield, S., Ferraro, T., Tomiyama, H., Hutson, J., Otvos, L., Jr., Tregear, G. W., Bathgate, R. A., and Wade, J. D. (2004) Synthesis, conformation, receptor binding, and biological activities of monobiotinylated human insulin-like peptide 3, *J. Pept. Res. 63*, 91−98.
29. Halls, M. L., Bond, C. P., Sudo, S., Kumagai, J., Ferraro, T., Layfield, S., Bathgate, R. A., and Summers, R. J. (2005) Multiple binding sites revealed by interaction of relaxin family peptides with native and chimeric relaxin family peptide receptors 1 and 2 (LGR7 and LGR8), *J. Pharmacol. Exp. Ther. 313*, 677−687.
30. Scott, D. S., Layfield, S., Riesewijk, A., Morita, H., Tregear, G., and Bathgate, R. (2004) The identification and characterisation of the mouse and rat relaxin receptors as the novel orthologs of human LGR7, *Clin. Exp. Pharmacol. Physiol. 31*, 828−832.
31. Scott, D. J., Fu, P., Shen, P. J., Gundlach, A., Layfield, S., Riesewijk, A., Tomiyama, H., Hutson, J. M., Tregear, G. W., and

Bathgate, R. A. (2005) Characterization of the rat INSL3 receptor, *Ann. N. Y. Acad. Sci. 1041*, 13−16.

32. van der Westhuizen, E. T., Sexton, P. M., Bathgate, R. A., and Summers, R. J. (2005) Responses of GPCR135 to human gene 3 (H3) relaxin in CHO-K1 cells determined by microphysiometry, *Ann. N. Y. Acad. Sci. 1041*, 332−337.

33. Sudo, S., Kumagai, J., Nishi, S., Layfield, S., Ferraro, T., Bathgate, R. A., and Hsueh, A. J. (2003) H3 relaxin is a specific ligand for LGR7 and activates the receptor by interacting with both the ectodomain and the exoloop 2, *J. Biol. Chem. 278*, 7855−7862.

34. Samuel, C. S., Unemori, E. N., Mookerjee, I., Bathgate, R. A., Layfield, S. L., Mak, J., Tregear, G. W., and Du, X. J. (2004) Relaxin modulates cardiac fibroblast proliferation, differentiation, and collagen production and reverses cardiac fibrosis *in vivo*, *Endocrinology 145*, 4125−4133.

35. McKinley, M. J., Burns, P., Colvill, L. M., Oldfield, B. J., Wade, J. D., Weisinger, R. S., and Tregear, G. W. (1997) Distribution of Fos immunoreactivity in the lamina terminalis and hypothalamus induced by centrally administered relaxin in conscious rats, *J. Neuroendocrinol. 9*, 431−437.

36. Paxinos, G., and Watson, C. (1986) *The Rat Brain in Stereotaxic Coordinates*, 2nd ed., Academic Press, Sydney, Australia.

37. Osheroff, P. L., and Phillips, H. S. (1991) Autoradiographic localization of relaxin binding sites in rat brain, *Proc. Natl. Acad. Sci. U.S.A. 88*, 6413−6417.

38. Tang, J. G., and Tsou, C. L. (1990) The insulin A and B chains contain structural information for the formation of the native molecule. Studies with protein disulphide-isomerase, *Biochem. J. 268*, 429−435.

39. Wade, J. D., and Tregear, G. W. (1997) Relaxin, *Methods Enzymol. 289*, 637−646.

40. Tang, J. G., Wang, Z. H., Tregear, G. W., and Wade, J. D. (2003) Human gene 2 relaxin chain combination and folding, *Biochemistry 42*, 2731−2739.

41. Bullesbach, E. E., and Schwabe, C. (1991) Total synthesis of human relaxin and human relaxin derivatives by solid-phase peptide synthesis and site-directed chain combination, *J. Biol. Chem. 266*, 10754−10761.

42. Akaji, K., Fujino, K., Tatsumi, T., and Kiso, Y. (1993) Total synthesis of human insulin by regioselective disulphide bond formation using the silyl chloride-sulfoxide method, *J. Am. Chem. Soc. 115*, 11384−11392.

43. Maruyama, K., Nagasawa, H., Isogai, A., Ishizaki, H., and Suzuki, A. (1992) Determination of disulfide bond arrangement in bombyxin-IV, an insulin superfamily peptide from the silkworm, *Bombyx mori*, by combination of thermolysin digestion of natural peptide and selective synthesis of disulfide bond isomers, *J. Protein Chem. 11*, 13−20.

44. Maruyama, K., Nagasawa, H., and Suzuki, A. (1999) 2,2′-Bispyridyl disulfide rapidly induces intramolecular disulfide bonds in peptides, *Peptides 20*, 881−884.

45. Lijnen, P. J., Petrov, V. V., and Fagard, R. H. (2000) Induction of cardiac fibrosis by transforming growth factor-β(1), *Mol. Genet. Metab. 71*, 418−435.

46. Aimes, R. T., and Quigley, J. P. (1995) Matrix metalloproteinase-2 is an interstitial collagenase. Inhibitor-free enzyme catalyzes the cleavage of collagen fibrils and soluble native type I collagen generating the specific 3/4- and 1/4-length fragments, *J. Biol. Chem. 270*, 5872−5876.

47. Zhao, L., Roche, P. J., Gunnersen, J. M., Hammond, V. E., Tregear, G. W., Wintour, E. M., and Beck, F. (1999) Mice without a functional relaxin gene are unable to deliver milk to their pups, *Endocrinology 140*, 445−453.

48. Du, X. J., Samuel, C. S., Gao, X. M., Zhao, L., Parry, L. J., and Tregear, G. W. (2003) Increased myocardial collagen and ventricular diastolic dysfunction in relaxin deficient mice: A gender-specific phenotype, *Cardiovasc. Res. 57*, 395−404.

49. Samuel, C. S., Zhao, C., Bathgate, R. A., Bond, C. P., Burton, M. D., Parry, L. J., Summers, R. J., Tang, M. L., Amento, E. P., and Tregear, G. W. (2003) Relaxin deficiency in mice is associated with an age-related progression of pulmonary fibrosis, *FASEB J. 17*, 121−123.

50. Samuel, C. S., Zhao, C., Bond, C. P., Hewitson, T. D., Amento, E. P., and Summers, R. J. (2004) Relaxin-1-deficient mice develop an age-related progression of renal fibrosis, *Kidney Int. 65*, 2054−2064.

51. Zhang, J., Qi, Y. F., Geng, B., Pan, C. S., Zhao, J., Chen, L., Yang, J., Chang, J. K., and Tang, C. S. (2005) Effect of relaxin on myocardial ischemia injury induced by isoproterenol, *Peptides 26*, 1632−1639.

52. Bittencourt, J. C., and Sawchenko, P. E. (2000) Do centrally administered neuropeptides access cognate receptors?: An analysis in the central corticotropin-releasing factor system, *J. Neurosci. 20*, 1142−1156.

53. Goto, M., Swanson, L. W., and Canteras, N. S. (2001) Connections of the nucleus incertus, *J. Comp. Neurol. 438*, 86−122.

54. Scott, D. J., Layfield, S., Riesewijk, A., Morita, H., Tregear, G. W., and Bathgate, R. A. D. (2005) Characterization of the mouse and rat relaxin receptors. *Ann. N.Y. Acad. Sci. 1041*, 8−12.

55. Rosengren, K. J., Lin, F., Bathgate, R. A. D., Tregear, G. W., Daly, N. L., Wade, J. D., and Craik, D. J. (2005) Solution structure and novel insights into the determinants of receptor specificity of human relaxin-3. *J. Biol. Chem.* (in press).